JDI Journal of Diabetes Investigation Open access
Official Journal of the Asian Association for the Study of Diabetes
ORIGINAL ARTICLE

MiR-488-3p facilitates wound healing through CYP1B1-mediated Wnt/β-catenin signaling pathway by targeting MeCP2

Chenchen Zuo*, Pengju Fan, Ying Yang, Chengjun Hu

Department of Plastic Surgery, Xiangya Hospital, Central South University, Changsha, Hunan, China

Keywords
CYP1B1, miR-488-3p, Wound healing

***Correspondence**
Chenchen Zuo
Tel.: +86-13875814146
E-mail address:
hucjxy@csu.edu.cn

J Diabetes Investig 2024; 15: 145–158

doi: 10.1111/jdi.14099

ABSTRACT

Introduction: Diabetic wounds are difficult to heal, but the pathogenesis is unknown. MicroRNAs (miRNAs) are thought to play important roles in wound healing. The effect of miR-488-3p in wound healing was studied in this article.

Materials and Methods: The gene methylation was measured by methylation specific PCR (MSP) assay. A dual-luciferase reporter assay was adopted to analyze the interaction between miR-488-3p and MeCP2.

Results: Cytochrome P450 1B1 (CYP1B1) is a monooxygenase belonging to the cytochrome P450 family that aids in wound healing. Our findings showed that the miR-488-3p and CYP1B1 expression levels were much lower in wound tissues of diabetics with skin defects, but the methyl-CpG-binding protein 2 (MeCP2) level was significantly higher than that in control skin tissues. MiR-488-3p overexpression increased cell proliferation and migration, as well as HUVEC angiogenesis, while inhibiting apoptosis, according to function experiments. *In vitro*, MeCP2 inhibited wound healing by acting as a target of miR-488-3p. We later discovered that MeCP2 inhibited CYP1B1 expression by enhancing its methylation state. In addition, CYP1B1 knockdown inhibited wound healing. Furthermore, MeCP2 overexpression abolished the promoting effect of miR-488-3p on wound healing. It also turned out that CYP1B1 promoted wound healing by activating the Wnt4/β-catenin pathway. Animal experiments also showed that miR-488-3p overexpression could accelerate wound healing in diabetic male SD rats.

Conclusions: MiR-488-3p is a potential therapeutic target for diabetic wound healing since it improved wound healing by activating the CYP1B1-mediated Wnt4/-catenin signaling cascade *via* MeCP2.

INTRODUCTION

Skin refers to the tissue that covers the surface of the human body and is in direct contact with the external environment, serving anti-friction and anti-infection functions. Skin injury is a common occurrence following an accident[1]. Wound healing consists of four processes: inflammation, cell proliferation, scar formation, and tissue regeneration, involving a variety of skin cells, including vascular endothelial cells, keratinocytes, and fibroblasts[2,3]. Delayed wound healing has long been a major public health concern, particularly among people with diabetes[4]. Approximately 15% of diabetic patients are at risk of developing non-healing ulcers[5]. According to reports, the cost of treating diabetic wounds is approximately $10 billion per year in the USA[6], imposing a huge burden on patients' lives. However, wound healing is a complicated process, and the mechanism involved is still unclear.

MicroRNAs (MiRNAs) refer to single-stranded non-coding RNAs with a length of 20–22 nt that participate in regulating many biological processes, including wound healing[5,7]. As proof, miR-497-5p expression in the skin wounds of diabetic mice was significantly lower than that in normal mice, and its upregulation accelerated wound healing[4]. In addition, miR-152-3p inhibition could enhance diabetic wound repair[8]. MiR-488-3p was

Received 12 June 2023; revised 15 September 2023; accepted 28 September 2023

previously confirmed as a target for the treatment of multiple diseases, including colorectal cancer[9] and panic disorder[10]. Notably, miR-488-3p overexpression could enhance the viability of osteoblasts and inhibit cell apoptosis, thereby promoting fracture healing[11]. Nevertheless, the function of miR-488-3p in regulating diabetic wound healing is largely unknown, which deserves to be further probed.

Methyl-CpG-binding protein 2 (MeCP2) inhibits the expression of downstream targets by binding to methylated DNA[12]. The role of MeCP2 in skin biology and diseases has been studied[13]. As proof, MeCP2 overexpression in fibroblasts could inhibit fibroblast proliferation and migration[14]. In addition, MeCP2 silencing was reported to enhance wound healing generated at sites of injury by promoting myofibroblast transdifferentiation[13]. However, the mechanism by which MeCP2 regulates wound healing has not been elucidated. Herein, it was predicted that miR-488-3p had potential binding sites to MeCP2 through TargetScan, StarBase, and miRDB.

Cytochrome P450 1B1 (CYP1B1) is a monooxygenase belonging to the cytochrome P450 family. Previously, elevation of CYP1B1 was detected in previously wounded and in dexpanthenol (a medication used extensively in clinical practice to enhance wound healing) -treated skin[15], indicating that CYP1B1 has a favorable influence on wound healing. Notably, CYP1B1 was the target of MeCP2 in regulating lung epithelial cell injury[16]; however, whether a similar regulatory relationship exists in wound healing remains to be further probed.

Herein, the function of miR-488-3p in regulating wound healing was probed. MiR-488-3p promoted wound healing through the CYP1B1-mediated Wnt4/β-catenin signaling pathway by targeting MeCP2. Our research provided a theoretical basis for the treatment of diabetic wound healing.

MATERIALS AND METHODS

Clinical samples collection

In conventional surgeries, wound tissues from diabetic patients with long-term skin defects were collected from the area around the lesion of the skin ulcer. The control group was composed of 30 patients who did not have diabetes but who had undergone an orthopedic operation for a non-traumatic disease. All samples were stored at −80°C for further examination. This study passed the review of the Ethics Committee of Xiangya Hospital of Central South University. All patients signed informed consent forms.

Cell culture and treatment

Human skin fibroblasts (HSF), keratinocytes (HaCaT), and human umbilical vein endothelial cells (HUVECs), purchased from ATCC (Manassas, VA, USA), were cultured in DMEM (Gibco, Carlsbad, CA, USA) containing 10% FBS (Gibco) at 37°C with 5% CO_2. For β-catenin inhibition, HSF cells and HUVECs were treated with a β-catenin inhibitor (JW 55, 5 μM) (Medchemexpress, Shanghai, China) for 24 h. For CYP1B1 inhibition, HSF cells and HUVECs were treated with a CYP1B1 inhibitor (CYP1B1-IN-1, 10 μM; Medchemexpress) for 24 h.

Cell transfection

GenePharma (Shanghai, China) provided the overexpression plasmid of MeCP2 (oe-MeCP2), the short hairpin RNA of CYP1B1 (sh-CYP1B1), the mimics or inhibitors of miR-488-3p, and the negative controls, which were transfected into cells with Lipofectamine™ 3000 (Invitrogen, Carlsbad, CA, USA).

Wound healing assay

The cells were cultured in 6-well plates (5×10^5 cells/well; Corning, Corning, NY, USA) for 12 h. After removing the medium, an artificial wound was created using a sterile pipette tip. The cells were washed and cultured, and images were taken at 0 and 24 h.

5-Bromo-2′-deoxyuridine (BrdU) assay

The cells were seeded onto 24-well plates and cultured for 4 h in a BrdU solution (10 μM; RiboBio, Guangzhou, China). The cells were rinsed three times with PBS before being fixed in 4% paraformaldehyde for 10 min to denature the DNA. The unspecific antigens were blocked using 1% bovine serum albumin. Then the cells were incubated with BrdU monoclonal antibody (ab6326, 1:300; Abcam, Cambridge, UK) overnight, followed by incubation with a secondary antibody (Beyotime, Shanghai, China) for 2 h. The nuclei were stained with DAPI (RiboBio), and the cells were observed by a fluorescent microscope.

Cell apoptosis assay

The cells were re-suspended in Annexin-binding buffer (500 μL; Beyotime) and stained for 10 min with Annexin V-FITC and PI dye before being subjected to flow cytometry (BD, San Diego, CA, USA).

Angiogenesis assay of HUVECs

HUVECs were seeded into 96-well plates (Corning) covered with Matrigel (1:1 dilution; BD, NJ, USA). The cells were grown in complete medium for 24 h after attachment. Angiogenesis was detected using a microscope (Nikon, Tokyo, Japan).

Real-time quantitative polymerase chain reaction (RT-qPCR)

Total RNA was extracted with TRIzol (ThermoFisher Scientific, Waltham, MA, USA). The 260/280 nm absorbance ratio was 1.7–1.8, demonstrating a good degree of purity. In addition, the integrity of RNA was analyzed by separating it on 1.0% agarose gel electrophoresis, stained with ethidium bromide and visualized under a gel documentation system (Bio-Rad, Hercules, CA, USA). If the 28S and 18S bands were bright, clear, and sharp, and the brightness of the 28S band was more than twice that of the 18S band, the quality of RNA was good. miRNAs were collected by the miRNA isolation kit (Takara, Osaka, Japan) and detected using a Taqman miRNA assay kit (Takara). The cDNA was synthesized with the reverse transcriptase kit (Toyobo, Tokyo, Japan) and subjected to RT-qPCR assay using SYBR (Thermo Fisher Scientific). GAPDH was used as the reference gene for MeCP2 and CYP1B1, and U6 was used as the reference

gene for miR-488-3p, miR-129-5p, miR-335-5p and miR-497-5p. The data were analyzed with the $2^{-\Delta\Delta C_T}$ method. The primers used in the study are listed as follows (5′–3′):

miR-129-5p (F): GATCCGCAAGCCCAGACCGCAAAAAGTTTTTA
miR-129-5p (R): AGCTTAAAAACTTTTTGCGGTCTGGGCTTGCG
miR-335-5p (F): TCAAGAGCAATAACGAAAAATGT
miR-335-5p (R): GCTGTCAACGATACGCTACGT
miR-497-5p (F): GTGCAGGGTCCGAGGT
miR-497-5p (R): TAGCCTGCAGCACACTGTGGT
miR-488-3p (F): CGGGGCAGCUCAGUACAG
miR-488-3p (R): CAGTGCGTGTCGTGGAGT
MeCP2 (F): TGACCGGGGACCCATGTAT
MeCP2 (R): CTCCACTTTAGAGCGAAAGGC
CYP1B1 (F): TGAGTGCCGTGTGTTTCGG
CYP1B1 (R): GTTGCTGAAGTTGCGGTTGAG
U6 (F): CGCTTCGGCAGCACATATAC
U6 (R): AAATATGGAACGCTTCACGA
GAPDH (F): AGGTCGGTGTGAACGGATTTG
GAPDH (R): TGTAGACCATGTAGTTGAGGTCA

Western blot

The proteins were isolated with RIPA, which were further transferred to a PVDF membrane (Millipore, Billerica, MA, USA). Then, the membranes were incubated with antibodies against MeCP2 (Abcam, 1:1,000, ab253197), CYP1B1 (Abcam, 1:1,000, ab185954), Wnt4 (Abcam, 1:1,000, ab262696), β-catenin (Abcam, 1:1,000, ab32572), and β-actin antibody (Abcam, 1:10,000, ab8226) overnight, then hybridized with a secondary antibody (Abcam, 1:10,000, ab7090) for 60 min. Blots were visualized by the GEL imaging system (Bio-Rad) and subsequently analyzed with ImageJ software.

Dual luciferase reporter assay

MeCP2 3′-untranslated region (UTR) fragments (total length: 2,376 bp) containing the miR-488-3p binding site were amplified by PCR. The resulting PCR products were subsequently digested with *Nhe I* and *Hind III* and cloned behind the firefly luciferase gene (reporter gene) into the pGL3-promoter Vector (SV40 promoter) (GenePharma). The location of the miR-488-3p binding site in the MECP2 3′ UTR was position 3,120–3,126, and the sequence was 5′-GCCUUUCAG-3′. Then, the cells were co-transfected with wt-MeCP2 or mut-MeCP2 plasmids and miR-488-3p mimics/inhibitor or mimics/inhibitor NC. The luciferase activity was determined according to the manufacturer's protocol using a dual-luciferase reporter assay system (Promega, Madison, WI, USA).

Methylation specific PCR

The location of the CpG island on CYP1B1 promoter is −1,810 ∼ −1,664 (chr2:c38077815-380770961). The sequence is listed as follows: 5′-GTGTGCACCACCACGTCCGGCTAACTTTTGTATTTTTAGTAGATGGGGTTTCGCCATGTTGGCCAGGCTGGTCTCGAACTCCTGACCTCAAGTGATCCGCCCGCTTAAGCCTCCCAAAGTGCTGGGATTACAGGCGTGAGCCACTG-3′. Genomic DNA was isolated using the DNA mini kit (Qiagen, Dusseldorf, Germany), and subjected to bisulfite. Methylation specific PCR (MSP) of bisulfite-transformed DNA was performed with a nested, two-stage PCR method as described previously[17]. The primer is listed as follows: F, 5′-TTGGGATTATAGGTGTGTATTATTA-3′; R, 5′-CCCAACACTTTAAAAAACTTAAAC-3′. The PCR products were analyzed by gel electrophoresis. The starting site of the left primer is 179 (size 25), and the starting site of the right primer is 316 (size: 24).

Construction of *in vivo* wound model

SJA Laboratory Animal Co., Ltd (Hunan, China) provided 24 male SD rats (8 weeks of age). This study passed the review of the Ethics Committee of Xiangya Hospital of Central South University. To develop diabetes, the rats were given an intraperitoneal injection of 50 mg/kg streptozotocin (STZ; Sigma-Aldrich, St Louis, MO, USA). After 48 h, if the blood glucose concentration of the rat was greater than or equal to 16.7 mmol/L, it was

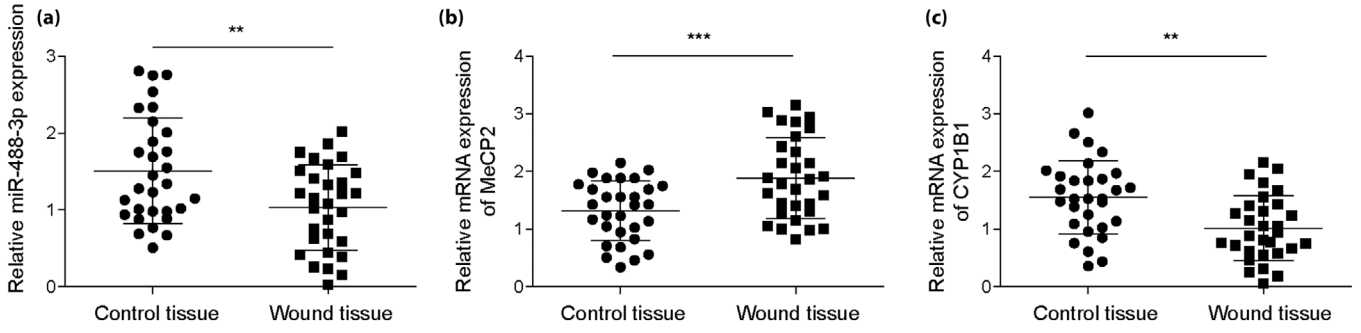

Figure 1 | miR-488-3p, MeCP2, and CYP1B1 expressions in wound tissues of diabetic with skin defect. (a) miR-488-3p expression in wound tissues of diabetic with skin defect and control skin tissues was determined using RT-qPCR. (b, c) MeCP2 and CYP1B1 levels in tissues were assessed by RT-qPCR. The data were expressed as mean ± SD. $n = 30$. $^{**}P < 0.01$, $^{***}P < 0.001$.

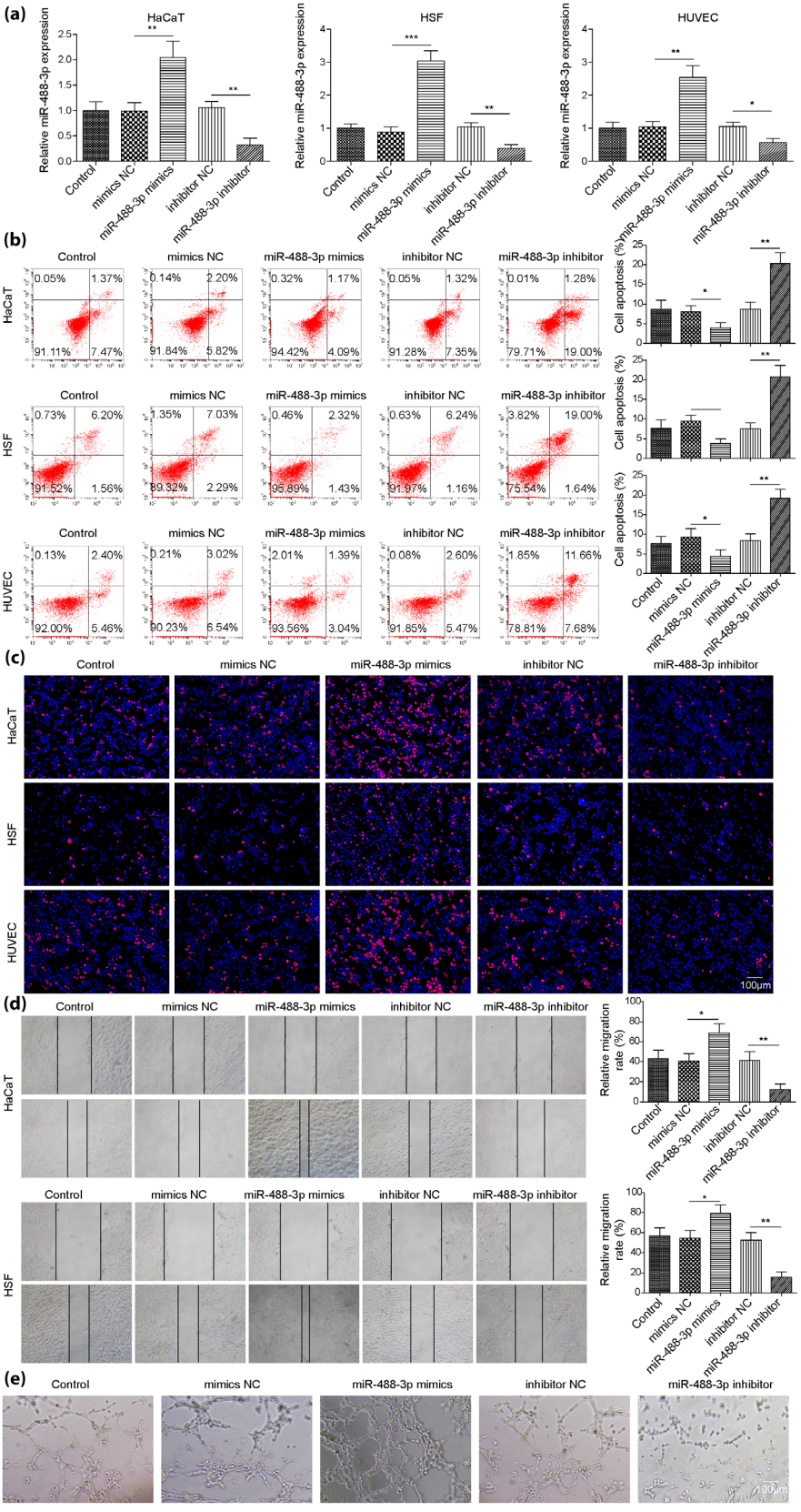

Figure 2 | miR-488-3p facilitated cell proliferation and migration as well as angiogenesis *in vitro*. MiR-488-3p mimics and inhibitor (20 nM) were transfected into HSF, HaCaT cells, and HUVECs. (a) miR-488-3p expression was detected using RT-qPCR. (b) Cell apoptosis of HSF, HaCaT cells and HUVECs was measured by a flow cytometry assay. (c) The BrdU assay was employed to analyze cell proliferation of HSF, HaCaT cells, and HUVECs (scale bar = 100 μm). (d) A wound healing assay was performed to determine cell migration of HSF and HaCaT cells. (e) *In vitro* angiogenesis assay was conducted to evaluate the angiogenesis ability of HUVECs (scale bar = 100 μm). The data were expressed as mean ± SD. All data were obtained from at least three replicate experiments. *$P < 0.05$, **$P < 0.01$, ***$P < 0.001$.

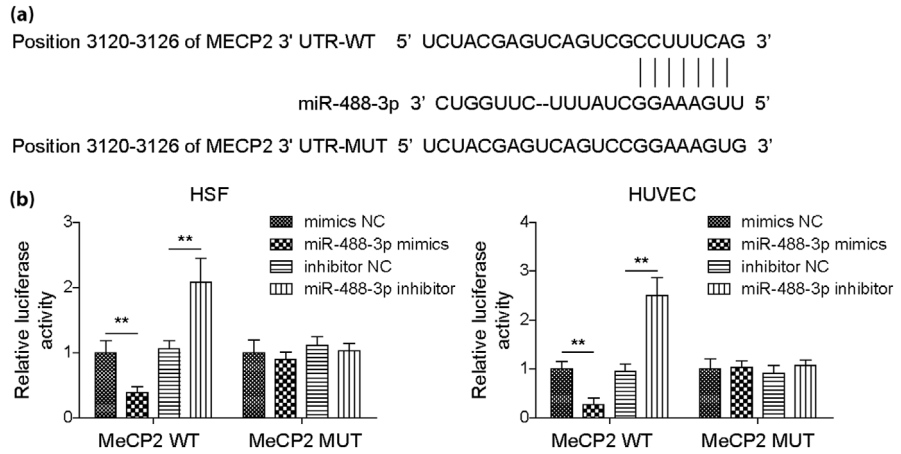

Figure 3 | MeCP2 was identified as the target of miR-488-3p. (a) Bioinformatics databases (TargetScan, StarBase and miRDB) were adopted to predict the binding site between miR-488-3p and MeCP2. (b) A dual-luciferase reporter assay was performed to analyze the interaction between miR-488-3p and MeCP2 in HSF cells and HUVECs. The data were expressed as mean ± SD. All data were obtained from at least three replicate experiments. **$P < 0.01$.

considered to have diabetes. A full-thickness skin wound in the diabetic rats was created as reported previously[18]. The diabetic rats were randomly divided into three groups: control group, ago-miR-NC (mimics NC) mimics group, and ago-miR-488-3p (miR-488-3p mimics) group (eight rats for each). Lentivirus (2×10^8 IFU/mL) harboring mimics NC or miR-488-3p mimics (purchased from Hanbio, Shanghai, China) were injected intradermally into the wound edges of rats. Wound images were acquired on days 0, 3, 7, and 11. Wound samples were collected 14 days after injury.

Hematoxylin–eosin staining

The skin tissue was fixed with 4% paraformaldehyde overnight and cut into 4 μm thick sections. Then the sections were dehydrated with gradient alcohol, washed, and embedded in paraffin. Following that, the sections were stained with hematoxylin–eosin (HE; Sigma-Aldrich). Sections were observed under a microscope (Nikon).

Masson staining of skin tissues

The skin tissue sections were stained with Weigert's hematoxylin (Solarbio, Beijing, China) and Masson's trichrome solution for 5 min, respectively. Sections were examined using a microscope (Nikon).

Data analysis

All the data were obtained from three independent experiments, analyzed by SPSS 19.0 (IBM, Armonk, NY, USA) and are presented as mean ± SD. Between-group differences and multi-group comparisons were determined using Student's *t*-test and one-way ANOVA, respectively. Values of *P* lower than 0.05 are referred to as significant.

RESULTS

miR-488-3p, MeCP2, and CYP1B1 expressions in wound tissues of diabetic with skin defect

We firstly observed that miR-488-3p expression was markedly lower in wound tissues of diabetic with a skin defect than that in control skin tissues (Figure 1a). In addition, the results from RT-qPCR revealed that MeCP2 expression was higher in wound tissues of diabetics with a skin defect than that in control skin tissues, while CYP1B1 was significantly lower in wound tissues of diabetics with a skin defect than that in control skin tissues (Figure 1b,c).

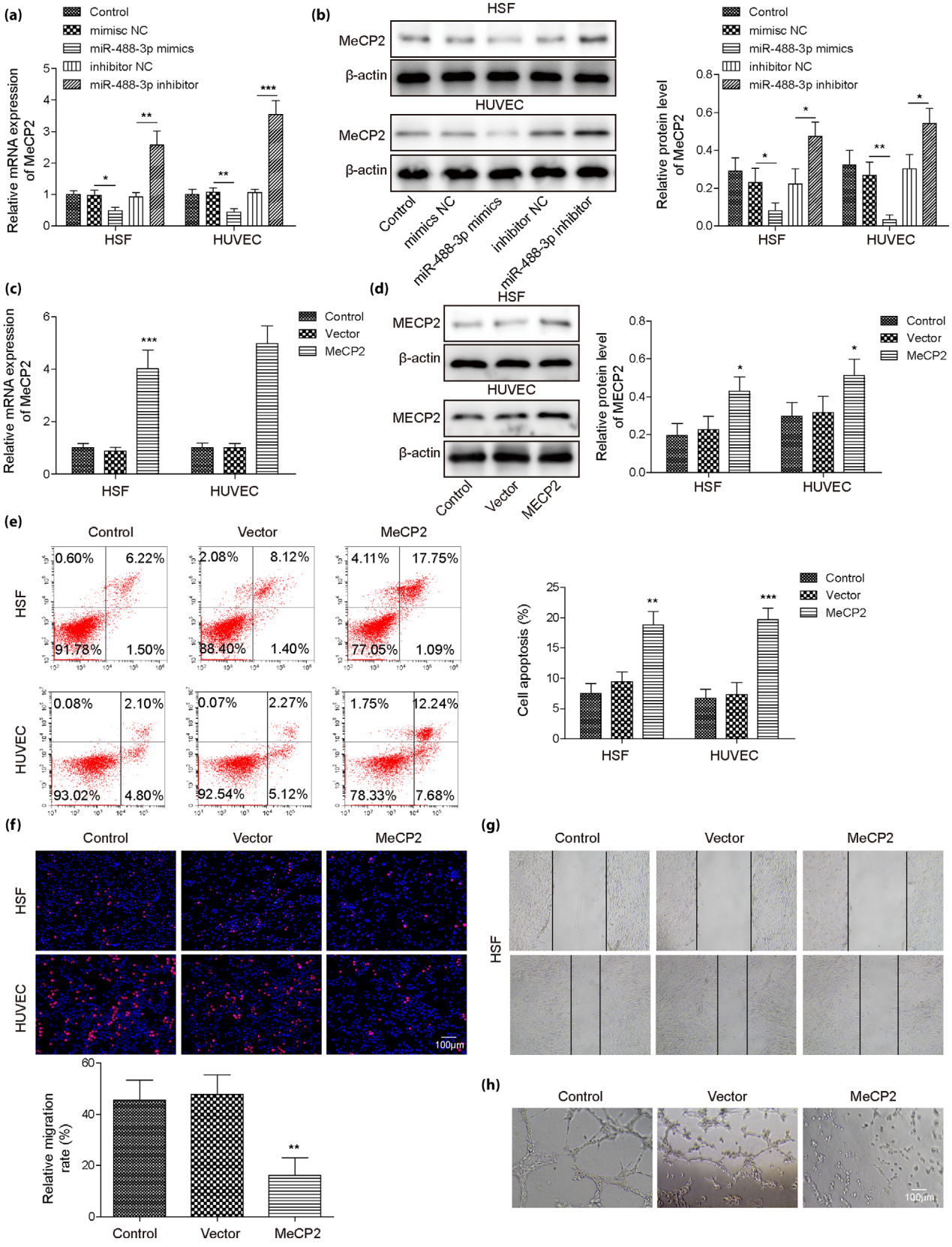

Figure 4 | MeCP2 overexpression suppressed cell proliferation and migration as well as angiogenesis. (a, b) RT-qPCR and western blot were adopted to examine MeCP2 expression in HSF cells and HUVECs transfected with miR-488-3p mimics or inhibitor (20 nM), respectively. MeCP2 overexpression was induced in HSF cells and HUVECs. (c, d) MeCP2 expression in cells was detected using RT-qPCR and western blot, respectively. (e) Flow cytometry assay was adopted to analyze cell apoptosis. (f) Cell proliferation was evaluated by BrdU assay (scale bar = 100 μm). (g) Wound healing assay was adopted to measure HSF cell migration. (h) The angiogenesis ability of HUVECs was determined using *in vitro* angiogenesis assay (scale bar = 100 μm). The data were expressed as mean ± SD. All data were obtained from at least three replicate experiments. *$P < 0.05$, **$P < 0.01$, ***$P < 0.001$.

miR-488-3p facilitated cell proliferation and migration as well as angiogenesis *in vitro*

As reported, endothelial cells, keratinocytes, and fibroblasts are all involved in the wound healing process[19]. To probe the potential role of miR-488-3p in wound healing, miR-488-3p overexpression and inhibition were induced in HSF, HaCaT cells, and HUVECs, and the cell behaviors and the angiogenic response of HUVECs were evaluated. Firstly, HSF cells and HUVECs were transfected with miR-488-3p mimics or mimics NC (20, 30, 50, and 100 nM), and it was observed that the levels of miR-488-3p were increased with increasing concentrations (Figure S1a). It was subsequently observed that miR-488-3p expression in HSF, HaCaT cells, and HUVECs was markedly reduced by miR-488-3p inhibitor (20 nM) transfection, while it was increased by miR-488-3p mimics (20 nM) transfection (Figure 2a), revealing the transfection to have been successful. The effect of miR-488-3p on miR-129-5p, miR-335-5p, and miR-497-5p levels in HUVECs was subsequently investigated. As shown in Figure S1b, the miR-129-5p, miR-335-5p, and miR-497-5p levels in HUVECs did not change significantly after miR-488-3p mimics or inhibitor transfection. As displayed in Figure 2b, the miR-488-3p inhibitor promoted cell apoptosis of HSF, HaCaT cells and HUVECs, while miR-488-3p overexpression presented the opposite effect. In addition, the proliferation of HSF, HaCaT cells, and HUVECs were markedly inhibited by miR-488-3p inhibitor, while they were promoted by miR-488-3p mimics (Figure 2c). Besides, miR-488-3p inhibitor repressed the migration of HSF and HaCaT cells, while miR-488-3p mimics promoted cell migration (Figure 2d). We then probed whether miR-488-3p could influence the angiogenesis of HUVECs, and the result displayed that miR-488-3p mimics transfection resulted in enhanced angiogenesis, while miR-488-3p inhibitor transfection led to reduced angiogenesis (Figure 2e).

MeCP2 functioned as the target of miR-488-3p

As is well known, miRNAs mediate post-transcriptional gene expressions by binding to their targets[20]. MiR-488-3p was predicted to have a binding site to MeCP2 using bioinformatics databases (TargetScan, StarBase, and miRDB), and the prediction results displayed that the location of the miR-488-3p binding site in the MECP2 3′ UTR was position 3,120–3,126 (Figure 3a). As shown in Figure 3b, the luciferase activity presented by wt-MeCP2 reporter was considerably reduced by miR-488-3p mimics (50 nM) and elevated by miR-488-3p inhibitor (50 nM), but miR-488-3p mimics or inhibitor had no effect on mut-MeCP2 reporter activity, suggesting that miR-488-3p directly targeted MeCP2. In conclusion, we identified MeCP2 as the target of miR-488-3p.

MeCP2 overexpression suppressed cell proliferation and migration as well as angiogenesis

Firstly, we observed that both MeCP2 expression in HSF cells and HUVECs was decreased by miR-488-3p mimics (50 nM) transfection and elevated by miR-488-3p inhibitor (50 nM) transfection (Figure 4a,b). To further probe the function of MeCP2 in wound healing, HSF cells and HUVECs were transfected with the overexpression plasmid of MeCP2 or empty vector. Firstly, HSF cells and HUVECs were transfected with the overexpression plasmid of MeCP2 or empty vector (100, 200, 300, and 400 ng/μL), and our results showed that the protein level of MeCP2 in HSF cells and HUVECs was increased with increasing plasmid concentrations (Figure S1c). As demonstrated in Figure 4c,d, transfection of the overexpression plasmid of MeCP2 markedly increased the MeCP2 expression in HSF cells and HUVECs. Functional experiments subsequently displayed that MeCP2 overexpression increased HSF cells and HUVEC apoptosis and reduced the proliferation (Figure 4e,f). In addition, MeCP2 overexpression resulted in reduced HSF cell migration and HUVEC angiogenesis (Figure 4g,h). In total, MeCP2 repressed wound healing.

MeCP2 suppressed cell proliferation and migration as well as angiogenesis through boosting CYP1B1 methylation

MeCP2 was reported previously to promote CYP1B1 methylation in lung epithelial cell injury[16], however, the regulatory relationship between MeCP2 and CYP1B1 in wound healing remained unknown. As shown in Figure 5a, the CYP1B1 level in HSF cells and HUVECs was significantly suppressed by MeCP2 overexpression. Interestingly, we observed that the methylation existed in the CYP1B1 promoter region (Figure S1d). The location of the CpG island on CYP1B1 promoter is −1,810 ∼ −1,664 (chr2: c38077815-380770961) (Figure S1d). And 5-Aza reduced the methylation in the CYP1B1 promoter region (Figure 5b). We also found that MeCP2 overexpression could promote CYP1B1 promoter methylation in HSF cells and HUVECs (Figure 5c). To

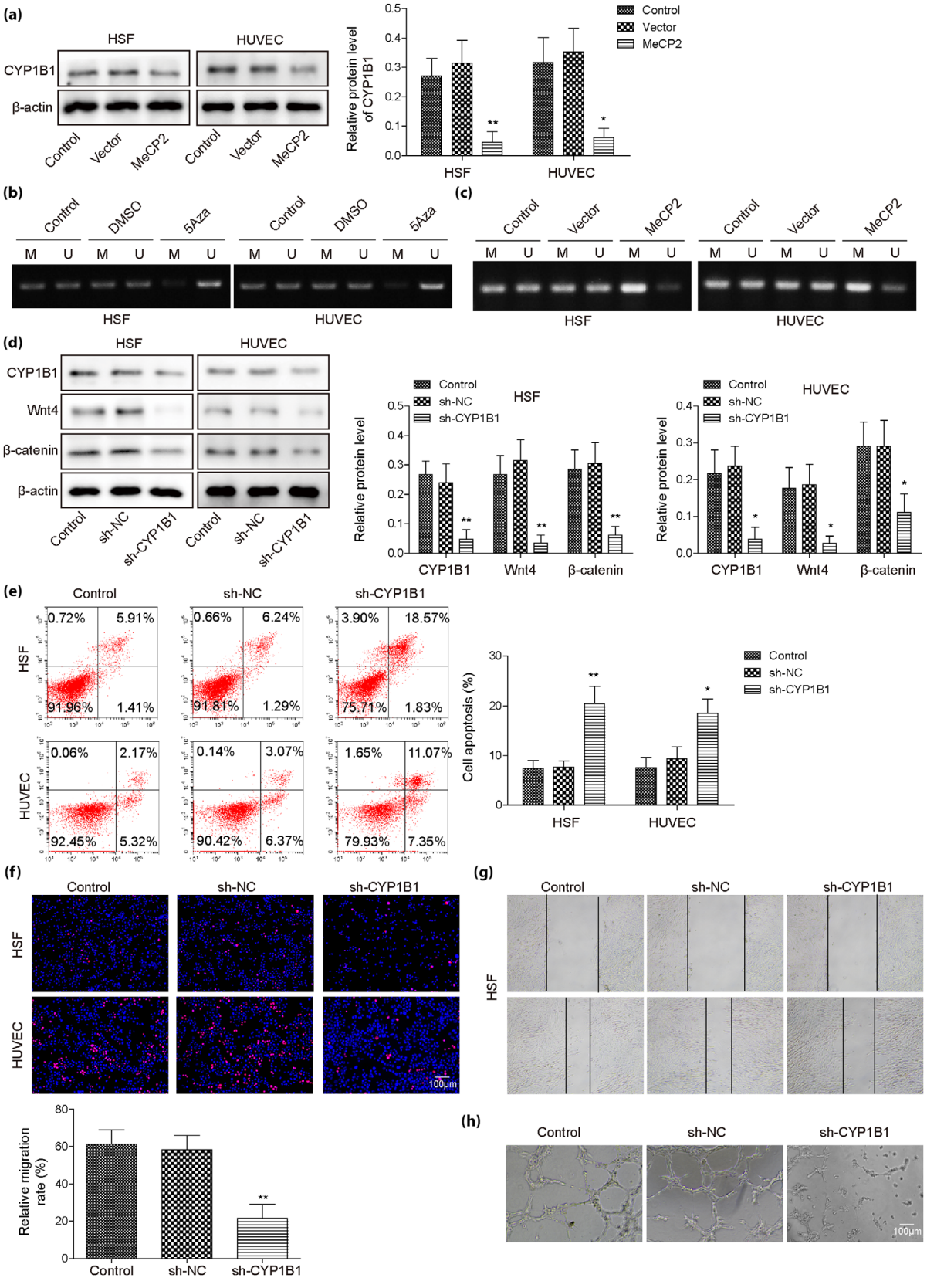

Figure 5 | MeCP2 suppressed cell proliferation, migration as well as angiogenesis through boosting CYP1B1 methylation. (a) CYP1B1 level in HSF cells and HUVECs after MeCP2 overexpression was assessed by western blot. (b) HSF cells and HUVECs were treated with 5Aza or DMSO, and CYP1B1 promoter methylation was assessed by MSP. (c) CYP1B1 promoter methylation was assessed by MSP in HSF cells and HUVECs with MeCP2 overexpression. HSF cells and HUVECs were transfected with sh-NC or sh-CYP1B1. (d) CYP1B1, Wnt4, and β-catenin levels were determined using western blot. (e) Flow cytometry was adopted to examine cell apoptosis. (f) The BrdU assay was employed to evaluate cell proliferation (scale bar = 100 μm). (g) Wound healing assay was adopted to analyze HSF cell migration. (h) The angiogenesis ability of HUVECs was determined using *in vitro* angiogenesis assay (scale bar = 100 μm). The data were expressed as mean ± SD. All data were obtained from at least three replicate experiments. $^{*}P < 0.05$, $^{**}P < 0.01$.

investigate the function of CYP1B1 in wound healing, sh-CYP1B1 was transfected into HSF cells and HUVECs, and we observed that CYP1B1 silencing resulted in the decreased protein level of CYP1B1 as well as reduced Wnt4 and β-catenin levels (Figure 5d). The results from the flow cytometry assay and BrdU assay showed that cell apoptosis was promoted following sh-CYP1B1 transfection, while cell proliferation was obviously repressed (Figure 5e,f). Additionally, the migratory ability of HSF cells was obviously inhibited following sh-CYP1B1 transfection (Figure 5g), and the angiogenic responses of HUVECs were markedly suppressed by CYP1B1 knockdown (Figure 5h). In summary, MeCP2 regulated cell proliferation, and apoptosis, HSF cell migration as well as HUVEC angiogenesis *via* regulation of CYP1B1 methylation.

miR-488-3p promoted cell proliferation and migration as well as angiogenesis through MeCP2-CYP1B1 axis-mediated Wnt4/β-catenin signaling pathway

To explore the potential function of miR-488-3p/MeCP2/CYP1B1 axis in wound healing, miR-488-3p mimics (20 nM) and/or MeCP2-overexpression vector were transfected into HSF cells and HUVECs. Firstly, we observed that miR-488-3p was markedly upregulated in miR-488-3p mimics + sh-NC group and miR-488-3p mimics + MeCP2 group compared with other groups (Figure 6a). It also turned out that miR-488-3p overexpression resulted in reduced MeCP2 levels and elevated CYP1B1, Wnt4, and β-catenin levels in HSF cells and HUVECs, while MeCP2 overexpression eliminated the effects of miR-488-3p mimics on these proteins (Figure 6b). In addition, cell apoptosis of HSF cells and HUVECs was inhibited after transfection with miR-488-3p mimics, while MeCP2 overexpression abolished this effect of miR-488-3p mimics (Figure 6c). Additionally, miR-488-3p overexpression significantly promoted cell proliferation, which was abolished by MeCP2 overexpression (Figure 6d). Moreover, the migration of HSF cells and angiogenesis of HUVECs was markedly promoted by miR-488-3p overexpression, while MeCP2 overexpression reversed the effect of miR-488-3p mimics (Figure 6e,f). To investigate the role of CYP1B1 and β-catenin in miR-488-3p-mediated biological effects during wound healing and tube formation, HSF cells and HUVECs were transfected with miR-488-3p mimics or miR-488-3p mimics combined with β-catenin inhibitor (JW 55) or CYP1B1 inhibitor (CYP1B1-IN-1) treatment. As revealed in Figure S2a, b, β-catenin inhibitor (JW 55) or CYP1B1 inhibitor (CYP1B1-IN-1) treatment could reverse the promoting effect of miR-488-3p overexpression on HSF cell migration and angiogenesis of HUVECs. In summary, miR-488-3p facilitates cell proliferation and migration as well as angiogenesis through the CYP1B1-mediated Wnt4/β-catenin signaling pathway by targeting MeCP2.

miR-488-3p accelerated wound healing *in vivo*

It was firstly observed that the change of miR-488-3p expression in the skin of control rats is not significant with time (Figure S1e). We observed decreased MeCP2 expression and increased miR-488-3p, CYP1B1 expressions in the skin of the rats injected with miR-488-3p mimics compared with controls (Figure 7a). Western blot analysis demonstrated that injection of miR-488-3p mimics lowered the MeCP2 level while increasing CYP1B1, Wnt4, and β-catenin levels in the skin of the rats (Figure 7b). It was observed that miR-488-3p upregulation accelerated wound healing in rats (Figure 7c). The findings of HE staining showed that the epidermis and dermis of the control rats were much thinner than those of the animals injected with miR-488-3p mimics (Figure 7d). In addition, we observed more wavy collagen fibers in skin of the rats injected with miR-488-3p mimics compared with controls (Figure 7e). Taken together, miR-488-3p overexpression accelerated wound closure *in vivo*.

DISCUSSION

As has been frequently demonstrated, miRNAs are abnormally expressed during wound healing[3]. Furthermore, miRNAs are being investigated as possible therapeutic targets in diabetic wound healing[21,22]. Herein, we found that miR-488-3p overexpression accelerated wound healing *in vitro* and *in vivo*. Mechanistically, miR-488-3p promoted CYP1B1-mediated Wnt4/β-catenin signaling pathway by targeting MeCP2. Therefore, our findings indicated that miR-488-3p had the potential to be a therapeutic target for diabetic wound healing.

Increasing evidence suggests that miRNAs are involved in regulating wound healing processes. For instance, Wang *et al.*[5] revealed that the topical administration of miR-129-5p and miR-335-5p overexpression enhanced wound healing in diabetic animals. Besides, miR-497-5p overexpression surrounding

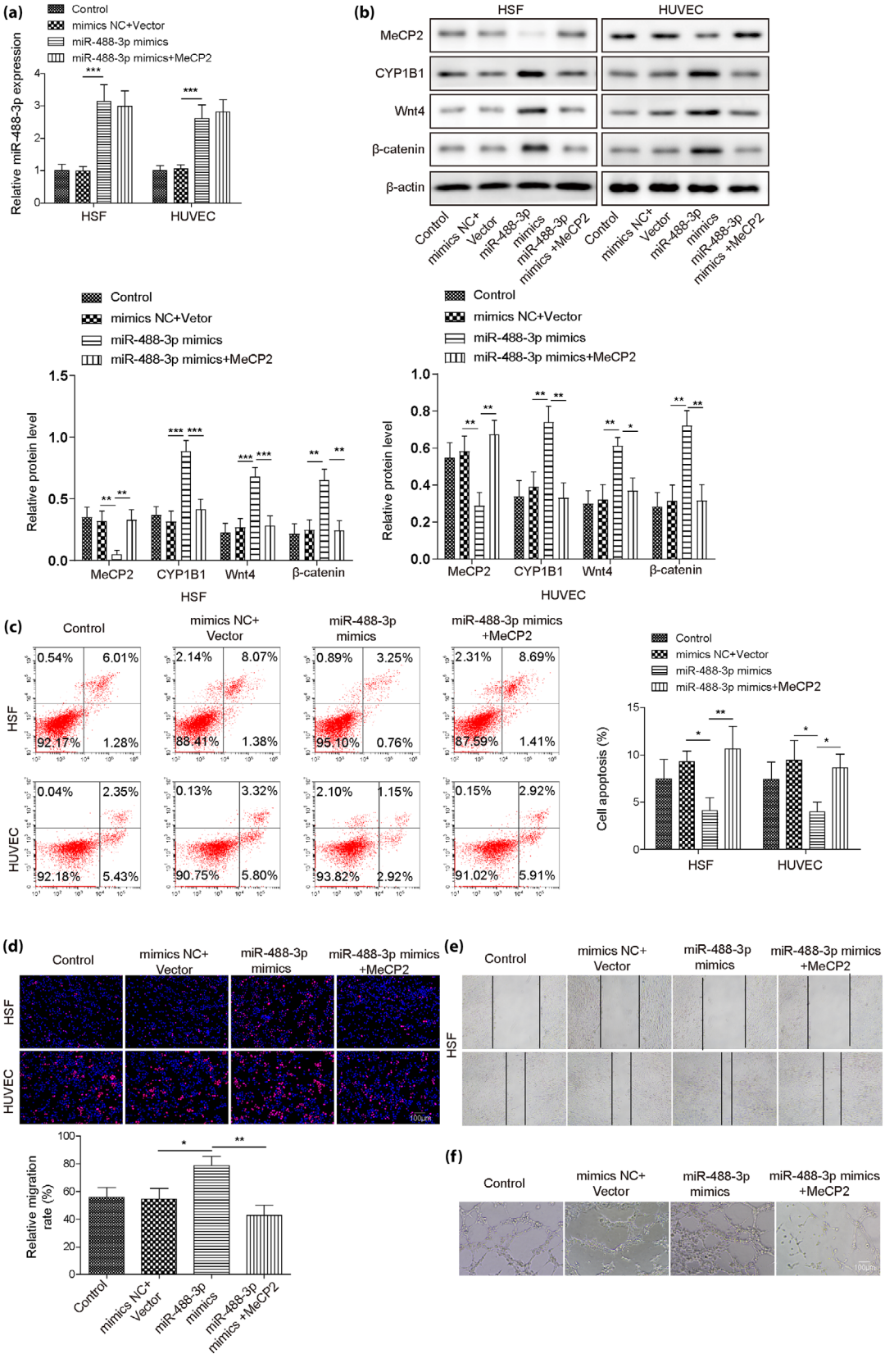

Figure 6 | miR-488-3p promoted cell proliferation and migration as well as angiogenesis through the MeCP2-CYP1B1 axis-mediated Wnt4/β-catenin signaling pathway. MiR-488-3p mimics (20 nM) and/or MeCP2-overexpression vector were transfected into HSF cells and HUVECs. (a) miR-488-3p expression was evaluated by RT-qPCR. (b) MeCP2, CYP1B1, Wnt4, and β-catenin levels were measured by western blot. (c) Flow cytometry was performed to assess cell apoptosis. (d) Cell proliferation was evaluated by BrdU assay (scale bar = 100 μm). (e) Wound healing assay was adopted to analyze migratory ability of HSF cells. (f) The angiogenesis ability of HUVECs was determined using the *in vitro* angiogenesis assay (scale bar = 100 μm). The data were expressed as mean ± SD. All data was obtained from at least three replicate experiments. *$P < 0.05$, **$P < 0.01$, ***$P < 0.001$.

wounds hastened wound closure in diabetic mice[4]. MiR-488-3p has already been identified as a tumor suppressor in a variety of malignancies[23,24]. The role of miR-488-3p in wound healing is poorly understood. In the current paper, we firstly observed that miR-488-3p was significantly lower in wound tissues of diabetic with a skin defect than that in control skin tissues, and its upregulation promoted HUVEC, HaCaT and HSF cell proliferation and migration as well as HUVEC angiogenesis *in vitro*, while inhibiting the apoptosis. In addition, miR-488-3p overexpression accelerated wound closure in diabetic mice. All the above results suggested that miR-488-3p presented beneficial effects in wound healing processes.

Next, we focused on downstream of miR-488-3p. By using bioinformatics databases and the dual-luciferase reporter assay, we found that miR-488-3p negatively regulated MeCP2 expression by directly binding to MeCP2. MeCP2, the Rett syndrome factor, is the prototypic methyl CpG-binding protein[25]. Recent research has proven the critical functions of MeCP2 in wound healing. As proof, MeCP2 overexpression in hepatic stellate cells could suppress critical genes determining the myofibroblast phenotype[13]. Given the importance of myofibroblasts in wound healing, MeCP2 has been proposed as a wound healing inhibitor[13]. MeCP2 overexpression has also been shown to disrupt a number of cellular activities during wound healing, including myofibroblast differentiation, fibroblast proliferation, and fibroblast migration[14]. Nevertheless, the interaction between miR-488-3p and MeCP2 in wound healing has not been elucidated. In the current study, function assays displayed that MeCP2 overexpression inhibited cell proliferation and HSF cell migration as well as HUVEC angiogenesis *in vitro*, while it promoted the apoptosis. Taken together, miR-488-3p promoted wound healing *via* directly interacting with MeCP2. It was observed that MeCP2 markedly inhibited CYP1B1 expression in HSF cells and HUVECs. It was reported previously that MeCP2 promoted CYP1B1 promoter methylation in epithelial cell injury[16]. However, the role of CYP1B1 in wound healing has not been reported before. Herein, we confirmed that MeCP2 suppressed CYP1B1 expression *via* promoting its methylation status in HSF cells and HUVECs. In addition, CYP1B1 knockdown inhibited cell proliferation and HSF cell migration as well as HUVEC angiogenesis *in vitro*, while promoting apoptosis. Moreover, MeCP2 overexpression abolished the promoting effects of miR-488-3p overexpression on cell proliferation and migration as well as angiogenesis *in vitro*. In conclusion, miR-488-3p might facilitate wound healing through CYP1B1 by targeting MeCP2.

Some studies have emphasized the role of Wnt/β-catenin signaling pathway in wound healing[26,27]. For instance, Ma *et al.*[28] demonstrated that mesenchymal stem cell-derived exosomes enhanced cell proliferation, migration, and inhibited cell apoptosis *via* activating Wnt/β-catenin signaling in cutaneous wound healing. As widely reported, the Wnt/β-catenin signaling pathway acts as the downstream pathway of CYP1B1 in regulating the development of various disease, such as breast carcinoma[29], cervical carcinoma[30], and PM2.5-induced cardiac developmental toxicity[31]. In addition, some studies have revealed that MeCP2 can directly regulate the Wnt/β-catenin pathway. As proof, Zhang *et al.*[32] revealed that MeCP2 may promote cell proliferation by regulating the Wnt/β-catenin pathway in oral squamous cell carcinoma (OSCC). In the current study, we found that miR-488-3p overexpression increased Wnt4 and β-catenin levels in HSF cells and HUVECs, which was eliminated by MeCP2 overexpression. Collectively, miR-488-3p promoted wound healing through activating CYP1B1-mediated Wnt4/β-catenin signaling pathway by targeting MeCP2. The possibility of whether MeCP2 can directly regulate the Wnt4/β-catenin pathway will be further explored in future studies.

Taken together, we verified the beneficial effect of miR-488-3p by overexpressing miR-488-3p to promote wound healing. Finally, we revealed a novel mechanism that the miR-488-3p/MeCP2/CYP1B1/Wnt4/β-catenin axis was involved in wound healing processes.

DISCLOSURE

All authors agree with the presented findings, have contributed to the work, and declare no conflict of interest.

Approval of the research protocol: This study was passed the review of the Clinical Medical Ethics Committee of Xiangya Hospital of Central South University.

Informed consent: All patients signed informed consent forms.

Registry and the registration no. of the study/trial: Approval date of Registry of the study is March 8, 2023 and the Registration No. is 2023030506.

Animal studies: This study was passed the review of the Animal Ethics Committee of Xiangya Hospital of Central South University.

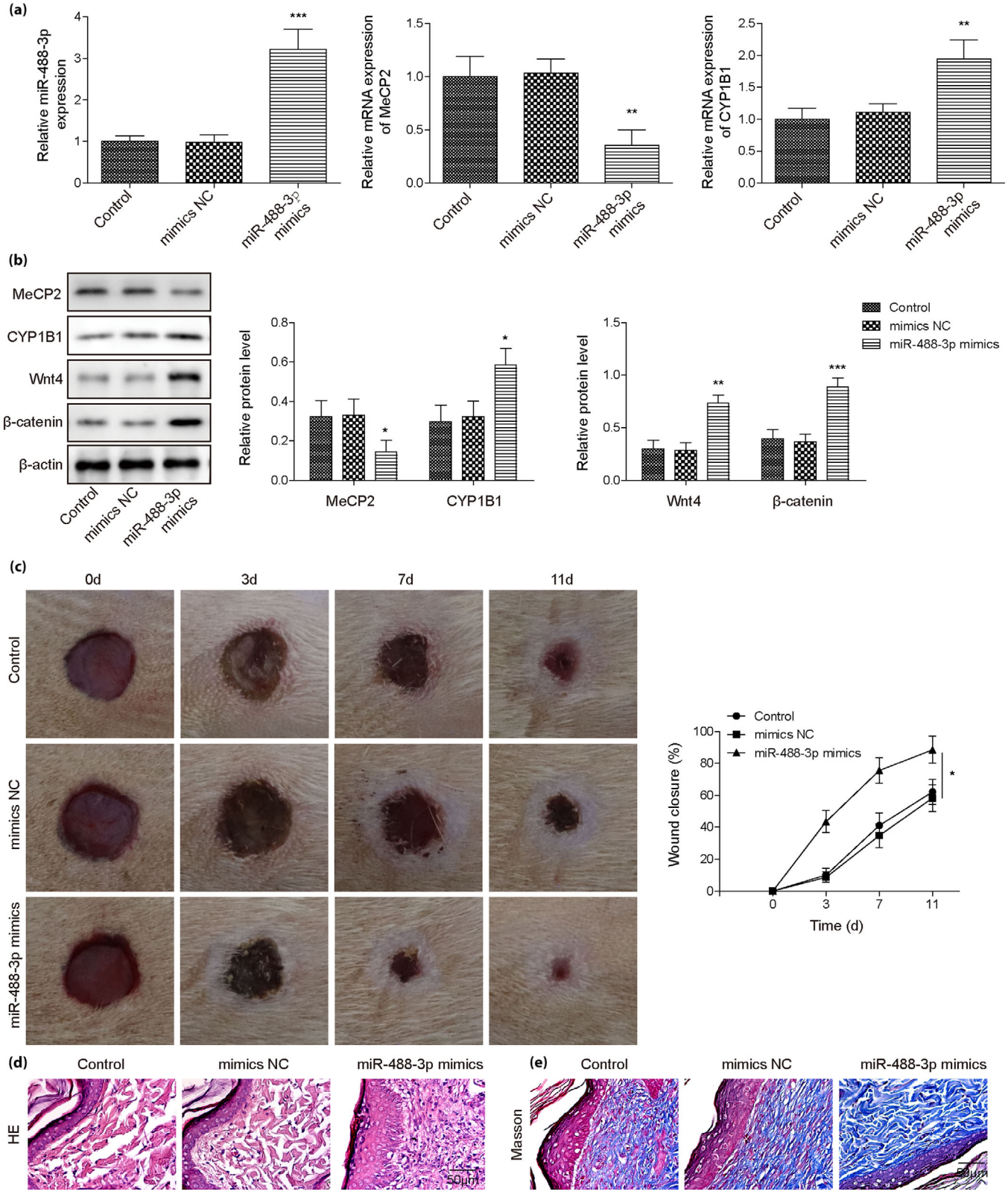

Figure 7 | miR-488-3p accelerated wound healing *in vivo*. We injected miR-488-3p mimics or mimics NC intradermally into the wound edges of diabetic rats after the skin was injured. (a) miR-488-3p, MeCP2, and CYP1B1 expressions in the skin of the rats were measured using RT-qPCR. (b) Western blot was employed to evaluate MeCP2, CYP1B1, Wnt4, and β-catenin levels in skin tissues. (c) Representative wound healing images, and the wound closures were quantified. (d, e) HE and Masson staining of skin tissues (scale bar = 50 μm). The data were expressed as mean ± SD. $n = 8$. *$P < 0.05$, **$P < 0.01$, ***$P < 0.001$.

REFERENCES

1. van Zanten MC, Mistry RM, Suami H, *et al*. The lymphatic response to injury with soft-tissue reconstruction in high-energy open tibial fractures of the lower extremity. *Plast Reconstr Surg* 2017; 139: 483–491.
2. Lewis CJ, Mardaryev AN, Poterlowicz K, *et al*. Bone morphogenetic protein signaling suppresses wound-induced skin repair by inhibiting keratinocyte proliferation and migration. *J Invest Dermatol* 2014; 134: 827–837.
3. Wang PH, Huang BS, Horng HC, *et al*. Wound healing. *J Chin Med Assoc* 2018; 81: 94–101.
4. Ban E, Jeong S, Park M, *et al*. Accelerated wound healing in diabetic mice by miRNA-497 and its anti-inflammatory activity. *Biomed Pharmacother* 2020; 121: 109613.
5. Wang W, Yang C, Wang X, *et al*. MicroRNA-129 and -335 promote diabetic wound healing by inhibiting Sp1-mediated MMP-9 expression. *Diabetes* 2018; 67: 1627–1638.
6. Raghav A, Khan ZA, Labala RK, *et al*. Financial burden of diabetic foot ulcers to world: a progressive topic to discuss always. *Ther Adv Endocrinol Metab* 2018; 9: 29–31.
7. Meng Z, Zhou D, Gao Y, *et al*. miRNA delivery for skin wound healing. *Adv Drug Deliv Rev* 2018; 129: 308–318.
8. Xu Y, Yu T, He L, *et al*. Inhibition of miRNA-152-3p enhances diabetic wound repair via upregulation of PTEN. *Aging (Albany NY)* 2020; 12: 14978–14989.
9. Deng X, Li D, Ke X, *et al*. Mir-488 alleviates chemoresistance and glycolysis of colorectal cancer by targeting PFKFB3. *J Clin Lab Anal* 2021; 35: e23578.
10. Muiños-Gimeno M, Espinosa-Parrilla Y, Guidi M, *et al*. Human microRNAs miR-22, miR-138-2, miR-148a, and miR-488 are associated with panic disorder and regulate several anxiety candidate genes and related pathways. *Biol Psychiatry* 2011; 69: 526–533.
11. Wang F, Hu XY, Cao C, *et al*. MiR-488 promotes fracture healing by targeting DKK1. *Eur Rev Med Pharmacol Sci* 2018; 22: 8965–8972.
12. Nan X, Ng HH, Johnson CA, *et al*. Transcriptional repression by the methyl-CpG-binding protein MeCP2 involves a histone deacetylase complex. *Nature* 1998; 393: 386–389.
13. Mann J, Oakley F, Akiboye F, *et al*. Regulation of myofibroblast transdifferentiation by DNA methylation and MeCP2: implications for wound healing and fibrogenesis. *Cell Death Differ* 2007; 14: 275–285.
14. He Y, Tsou PS, Khanna D, *et al*. Methyl-CpG-binding protein 2 mediates antifibrotic effects in scleroderma fibroblasts. *Ann Rheum Dis* 2018; 77: 1208–1218.
15. Heise R, Skazik C, Marquardt Y, *et al*. Dexpanthenol modulates gene expression in skin wound healing in vivo. *Skin Pharmacol Physiol* 2012; 25: 241–248.
16. Lin J, Peng J, Liu G, *et al*. Overexpression of MECP2 attenuates cigarette smoke extracts induced lung epithelial cell injury by promoting CYP1B1 methylation. *J Toxicol Sci* 2020; 45: 177–186.
17. Lu C, Wei Y, Wang X, *et al*. DNA-methylation-mediated activating of lncRNA SNHG12 promotes temozolomide resistance in glioblastoma. *Mol Cancer* 2020; 19: 28.
18. Yang C, Zhu P, Yan L, *et al*. Dynamic changes in matrix metalloproteinase 9 and tissue inhibitor of metalloproteinase 1 levels during wound healing in diabetic rats. *J Am Podiatr Med Assoc* 2009; 99: 489–496.
19. Lin H, Zheng Z, Yuan J, *et al*. Collagen peptides derived from *Sipunculus nudus* accelerate wound healing. *Molecules* 2021; 26: 1385.
20. Ambros V. The functions of animal microRNAs. *Nature* 2004; 431: 350–355.
21. Eissa S, Matboli M, Bekhet MM. Clinical verification of a novel urinary microRNA panal: 133b, -342 and -30 as biomarkers for diabetic nephropathy identified by bioinformatics analysis. *Biomed Pharmacother* 2016; 83: 92–99.
22. Ashoori MR, Rahmati-Yamchi M, Ostadrahimi A, *et al*. MicroRNAs and adipocytokines: promising biomarkers for pharmacological targets in diabetes mellitus and its complications. *Biomed Pharmacother* 2017; 93: 1326–1336.
23. Zhao Y, Lu G, Ke X, *et al*. miR-488 acts as a tumor suppressor gene in gastric cancer. *Tumour Biol* 2016; 37: 8691–8698.
24. Guo JY, Wang XQ, Sun LF. MicroRNA-488 inhibits ovarian cancer cell metastasis through regulating CCNG1 and p53 expression. *Eur Rev Med Pharmacol Sci* 2020; 24: 2902–2910.
25. Amir RE, van den Veyver IB, Wan M, *et al*. Rett syndrome is caused by mutations in X-linked MECP2, encoding methyl-CpG-binding protein 2. *Nat Genet* 1999; 23: 185–188.
26. Yang HL, Tsai YC, Korivi M, *et al*. Lucidone promotes the cutaneous wound healing process via activation of the PI(3)K/AKT, Wnt/β-catenin and NF-κB signaling pathways. *Biochim Biophys Acta Mol Cell Res* 2017; 1864: 151–168.
27. Lu T, Bao Z, Wang Y, *et al*. Karyopherinβ1 regulates proliferation of human glioma cells via Wnt/β-catenin pathway. *Biochem Biophys Res Commun* 2016; 478: 1189–1197.
28. Ma T, Fu B, Yang X, *et al*. Adipose mesenchymal stem cell-derived exosomes promote cell proliferation, migration, and

inhibit cell apoptosis via Wnt/β-catenin signaling in cutaneous wound healing. *J Cell Biochem* 2019; 120: 10847–10854.
29. Lei T, Zhang W, He Y, *et al*. ZNF276 promotes the malignant phenotype of breast carcinoma by activating the CYP1B1-mediated Wnt/β-catenin pathway. *Cell Death Dis* 2022; 13: 781.
30. Park YS, Kwon YJ, Chun YJ. CYP1B1 activates Wnt/β-catenin signaling through suppression of Herc5-mediated ISGylation for protein degradation on β-catenin in HeLa cells. *Toxicol Res* 2017; 33: 211–218.
31. Yue C, Ji C, Zhang H, *et al*. Protective effects of folic acid on PM2.5-induced cardiac developmental toxicity in zebrafish embryos by targeting AhR and Wnt/β-catenin signal pathways. *Environ Toxicol* 2017; 32: 2316–2322.
32. Zhang N, Wei ZL, Yin J, *et al*. MiR-106a* inhibits oral squamous cell carcinoma progression by directly targeting MeCP2 and suppressing the Wnt/β-catenin signaling pathway. *Am J Transl Res* 2018; 10: 3542–3554.

SUPPORTING INFORMATION

Additional supporting information may be found online in the Supporting Information section at the end of the article.

Figure S1 | (a) HSF cells and HUVECs were transfected with miR-488-3p mimics or mimics NC (20, 30, 50, and 100 nM), and the miR-488-3p expression in HSF cells and HUVECs was examined by RT-qPCR. (b) miR-129-5p, miR-335-5p, and miR-497-5p levels in HUVECs after miR-488-3p mimics or inhibitor transfection were detected by RT-qPCR. (c) HSF cells and HUVECs were transfected with the overexpression plasmid of MeCP2 or empty vector (100, 200, 300, and 400 ng/μL), and the MeCP2 protein level in cells was examined by western blot. (d) The location of the CpG island on CYP1B1 promoter was presented. (e) miR-488-3p expression in the skin of control rats at 0, 3, 7, and 11 days was analyzed by RT-qPCR ($N = 8$). The data were expressed as mean ± SD. All data were obtained from at least three replicate experiments. $^{*}P < 0.05$, $^{**}P < 0.01$, $^{***}P < 0.001$.

Figure S2 | HSF cells and HUVECs were transfected with miR-488-3p mimics or miR-488-3p mimics combined with β-catenin inhibitor (JW 55) or CYP1B1 inhibitor (CYP1B1-IN-1) treatment. (a) Wound healing assay was adopted to analyze the migratory ability of HSF cells. (b) The angiogenesis ability of HUVECs was determined using an *in vitro* angiogenesis assay (scale bar = 100 μm). The data were expressed as mean ± SD. All data were obtained from at least three replicate experiments. $^{*}P < 0.05$, $^{**}P < 0.01$.